

The Central kpc of Starbursts and AGN
ASP Conference Series, Vol. xxx, 2001
J. H. Knapen, J. E. Beckman, I. Shlosman, and T. J. Mahoney

Relationship of Black Holes to Bulges

David Merritt and Laura Ferrarese

Department of Physics and Astronomy, Rutgers University, New Brunswick, NJ, USA

Abstract. Supermassive black holes appear to be uniquely associated with galactic bulges. The mean ratio of black hole mass to bulge mass was until recently very uncertain, with ground based, stellar kinematical data giving a value for $\langle M_\bullet/M_{\text{bulge}} \rangle$ roughly an order of magnitude larger than other techniques. The discrepancy was resolved with the discovery of the $M_\bullet - \sigma$ relation, which simultaneously established a tight correlation between black hole mass and bulge velocity dispersion, and confirmed that the stellar kinematical mass estimates were systematically too large due to failure to resolve the black hole's sphere of influence. There is now excellent agreement between the various techniques for estimating $\langle M_\bullet/M_{\text{bulge}} \rangle$, including dynamical mass estimation in quiescent galaxies; reverberation mapping in active galaxies and quasars; and computation of the mean density of compact objects based on integrated quasar light. All techniques now give $\langle M_\bullet/M_{\text{bulge}} \rangle \approx 10^{-3}$ and $\rho_\bullet \approx 3 \times 10^5 M_\odot/\text{Mpc}^{-3}$. Implications of the $M_\bullet - \sigma$ relation for the formation of black holes are discussed.

1. Introduction

The argument that active galaxies and quasars are powered by accretion onto massive compact objects was first made almost four decades ago (Salpeter 1964; Zeldovich 1964). Since that time, the existence of supermassive black holes has been confirmed in the nuclei of nearby galaxies and in a handful of more distant galaxies by direct dynamical measurement of their masses. The best determinations are in our own Galaxy ($M_\bullet \approx 3 \times 10^6 M_\odot$, Genzel *et al.* 2000; Ghez *et al.* 1998), NGC 4258 (Miyoshi *et al.* 1995), and M87 (Macchetto *et al.* 1997). The data for each of these galaxies exhibit a clear rise very near the center in the orbital velocity of stars or gas, suggestive of motion around a compact object. Data of this quality are unfortunately still rare, and the majority of black hole detections have necessarily been based on stellar-kinematical data from galaxies which do not yield a clear signature of the presence of a black hole. These data (Magorrian *et al.* 1998; Richstone *et al.* 1998) imply a mean black hole mass that is uncomfortably large compared with values predicted from quasar light. The inconsistency has been taken as evidence for low radiative efficiencies during the optically bright phase of quasars (e.g. Haehnelt, Natarajan & Rees 1998) or for continued growth of black holes after the quasar epoch (e.g. Richstone *et al.* 1998).

It is now clear that this discrepancy was due to almost entirely to systematic errors in the stellar kinematical mass estimates. The first convincing demonstration of this came from the $M_\bullet - \sigma$ relation, a tight empirical correlation between black hole mass and bulge velocity dispersion. The $M_\bullet - \sigma$ relation was discovered by ranking black hole detections in terms of their believability and excluding the least secure cases. The remarkable and unexpected result (Ferrarese & Merritt 2000) was an almost perfect correlation between M_\bullet and σ for the best-determined black hole masses, compared to a much weaker correlation for the less secure masses. Ground based, stellar kinematical estimates of M_\bullet were found to scatter above the $M_\bullet - \sigma$ relation by as much as two orders of magnitude, suggesting that many of the published masses were spurious and that most were substantial overestimates.

The ability of the $M_\bullet - \sigma$ relation to “separate the wheat from the chaff” has led to a rapid advance in our understanding of black hole demographics. We review that progress in §2 and §3; we argue that there is now almost embarrassingly good agreement between the results from the various techniques for estimating the mean mass density of black holes in the universe. Black hole masses determined dynamically in nearby quiescent galaxies are now fully consistent with masses inferred in active galaxies and quasars, and with estimates of the mean density of dark relic objects produced by accretion during the quasar epoch. The need for non-standard accretion histories in order to reproduce a large density of black holes in the current universe has disappeared.

A recurring theme in this review is the importance of adequate data when detecting black holes and estimating their masses. When the first black hole detections were being published, there was much discussion about whether the observations (all ground based at the time) were of sufficient quality to resolve the black holes’ sphere of influence, $r_h = GM_\bullet/\sigma^2$, in the galaxies where detections had been claimed. We now know that the ground based data almost always failed to do this, sometimes by a large factor, and that this failure led to substantial, systematic overestimates of M_\bullet (§2). The situation has improved somewhat with the Space Telescope, but not dramatically: we argue (§4) that the number of galaxies with secure dynamical estimates of M_\bullet will increase only modestly over the next few years in spite of ambitious ongoing programs with HST. This is partly due to the fact that these observations were planned at a time when the mean black hole mass was believed to be much larger than it is now. Progress in our understanding of black hole demographics is more likely to come from techniques with higher effective resolution than stellar or gas kinematics, notably reverberation mapping in AGN (Peterson 1993).

While the ability of the $M_\bullet - \sigma$ relation to clarify the data has been an enormous boon, the existence of such a tight correlation must also be telling us something fundamental about the way in which black holes form and about the connection between black holes and bulges. Unfortunately, the theoretical understanding of this connection has lagged behind the phenomenology. We summarize the proposed explanations for the origin of the $M_\bullet - \sigma$ relation in §5 and discuss their strengths and weaknesses.

2. Black Hole Mass Estimates: a Critical Review

Epimetheus: Wie vieles ist denn dein?

Prometheus: Der Kreis, den meine Wirksamkeit erfüllt!

Epimetheus: What then do you possess?

Prometheus: My sphere of influence - nothing more and nothing less!

Goethe, Prometheus

2.1. A Discrepancy, and its Resolution

By 1999, a clear discrepancy was emerging between black hole masses derived from stellar kinematical studies and most other techniques. The former sample included many “standard bearers” like M31 (Richstone, Bower & Dressler 1990), NGC 3115 (Kormendy *et al.* 1996a) and NGC 4594 (Kormendy *et al.* 1996b). The size of the discrepancy was difficult to pin down since there were (and still are) essentially no galaxies for which black hole masses had been independently derived using more than one technique. However the masses derived from ground based stellar kinematics were much larger, by roughly an order of magnitude on average, than those inferred from other techniques when galaxies with similar properties were compared, or when estimates of the cosmological density of black holes or the mean ratio of black hole mass to bulge mass were made. The discrepancy was clearest in two arenas:

- *Active vs. Quiescent Galaxies.* In Seyfert galaxies, the gravitational influence of the black hole can be measured on small scales, $\sim 10^{-2}$ pc, using emission lines from the broad emission line region (BLR). The technique of “reverberation mapping” combines the velocity of the BLR gas with an estimate of the size of the BLR based on time delay measurements (Peterson 1993). Reverberation mapping masses have been derived for about three dozen black holes (Wandel, Peterson & Malkan 1999; Kaspi *et al.* 2000). These masses fall a factor of 5-20 below the $M_\bullet - L_{\text{bulge}}$ relation defined by ground based, stellar kinematical data (Wandel 1999, 2000).
- *Quasar Light vs. Black Hole Demographics.* The mass density of black holes at large redshifts can be estimated by requiring the optical QSO luminosity function to be reproduced by accretion onto black holes (Soltan 1982). Assuming a standard accretion efficiency of $\sim 10\%$, the mean mass density in black holes works out to be $\rho_\bullet \sim 2 \times 10^5 M_\odot \text{Mpc}^{-3}$ (Chokshi & Turner 1992; Salucci *et al.* 1999). A similar argument based on the X-ray background gives consistent results, $\rho_\bullet \sim 3 \times 10^5 M_\odot \text{Mpc}^{-3}$ (Fabian & Iwasawa 1999; Salucci *et al.* 1999). By comparison, the black hole mass density implied by stellar kinematical modelling was about ten times higher (Magorrian *et al.* 1998; Richstone *et al.* 1998; Faber 1999).

Serious inconsistencies like these only appeared when comparisons were made with black hole masses derived from the stellar kinematical data; all other techniques gave roughly consistent values for ρ_\bullet and $\langle M_\bullet/M_{\text{bulge}} \rangle$. Nevertheless, most authors accepted the correctness of the stellar dynamical mass estimates and looked elsewhere to explain the discrepancies. Ho (1999) suggested that the

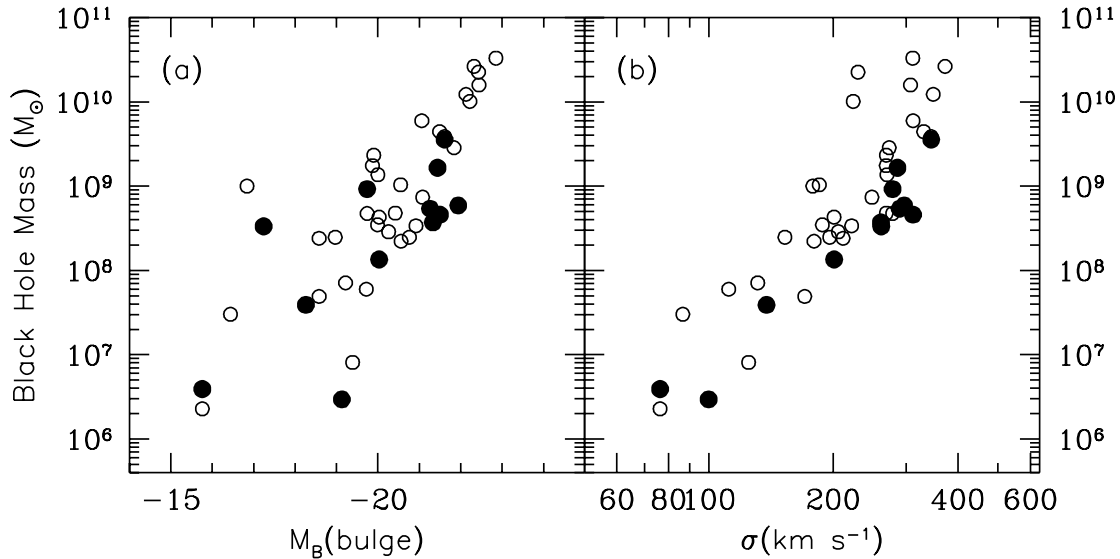


Figure 1. Discovery of the M_{\bullet} – σ relation (adapted from Ferrarese & Merritt 2000). (a) M_{\bullet} vs. bulge luminosity; (b) M_{\bullet} vs. bulge velocity dispersion. “Sample A” masses, derived from high quality data, are indicated with filled circles; “Sample B” masses, from lower quality data, are the open circles.

reverberation mapping masses had been systematically underestimated. Wandel (1999) proposed that black holes in active galaxies were smaller on average than those in quiescent galaxies, due either to different accretion histories or to selection effects. Richstone *et al.* (1998) and Faber (1999) suggested that the inconsistency between their group’s masses and the masses inferred from quasar light could be explained if black holes had acquired 80% of their mass *after* the quasar epoch through some process that produced no observable radiation.

What particularly caught our attention was the gulf between black hole masses derived from high- and low-resolution data, and (to a lesser extent) between gas- and stellar dynamical data; the former (e.g. Ferrarese, Ford & Jaffe 1996; Ferrarese & Ford 1999) were typically taken at higher resolution than the latter. Black hole masses derived from the highest resolution data, in galaxies like the Milky Way (Ghez *et al.* 1998; Genzel *et al.* 2000) and M87 (Macchetto *et al.* 1997), were the *smallest* when expressed as a fraction of the bulge mass, with $M_{\bullet}/M_{\text{bulge}} \approx 10^{-3}$. The *largest* fractional black hole masses – in galaxies like NGC 3377 (Kormendy *et al.* 1998) or NGC 4486b (Kormendy *et al.* 1997) – were mostly derived from stellar absorption-line spectra obtained from the ground, at resolutions of $\sim 1''$, corresponding to typical linear scales of 10 – 100 pc. The mean value of $M_{\bullet}/M_{\text{bulge}}$ for these galaxies was claimed to be about 10^{-2} (Magorrian *et al.* 1998; Richstone *et al.* 1998), roughly an order of magnitude greater than the value derived from the high-resolution data. We began to suspect that some of the masses derived from the lower-quality data might be serious over-estimates – or, even worse, that some of the “detections” based on these data were spurious.

To test this hypothesis, we tabulated all of the published black hole masses that had been derived from stellar- or gas kinematical data (excluding the reverberation mapping masses) and divided them into two groups based on their expected accuracy. This is not quite as easy as it sounds, since the “accuracy” of a black hole mass estimate is not necessarily related in any simple way to its published confidence range. Our criterion was simply the quality of the data: “accurate” black hole masses were those derived from HST data, at resolutions of $\sim 0.1''$, as well as M_\bullet for the Milky Way black hole (which is by far the nearest) and in NGC 4258 (for which VLBI gives a resolution of ~ 0.1 pc). The velocity data for these galaxies (our “Sample A”) was always found to exhibit a clear rise in the inner few data points, suggesting that the black hole’s sphere of influence $r_h \equiv GM_\bullet/\sigma^2$ had been well resolved. The remaining black hole masses (“Sample B”) were all those derived from lower-resolution data, typically ground-based stellar kinematics, including most of the masses in the Magorrian *et al.* (1998) study. Sample A contained 12 galaxies, Sample B 28.

Our first attempt to compare “Sample A” and “Sample B” masses was disappointing (Figure 1a). In the $M_\bullet - L_{\text{bulge}}$ plane, the Sample A masses do fall slightly below those from Sample B, but the intrinsic scatter in L_{bulge} is apparently so large that there is no clear difference in the relations defined by the two samples.

But when we plotted M_\bullet versus the velocity dispersion σ of the bulge stars, something magical happened (Figure 1b): now the Sample A galaxies clearly defined the *lower edge* of the relation, while the Sample B galaxies scattered above, some by as much as two orders of magnitude in M_\bullet ! Furthermore the correlation defined by the Sample A galaxies alone was very tight.

What particularly impressed us about the $M_\bullet - \sigma$ plot was the fact that the Sample A galaxies, which are diverse in their properties, showed such a tight correlation; while the Sample B galaxies, which are much more homogeneous, exhibited a large scatter. For instance, Sample A contains two spiral galaxies, two lenticulars, and both dwarf and giant ellipticals; while the Sample B galaxies are almost exclusively giant ellipticals. Furthermore the black hole masses in Sample A were derived using a variety of techniques, including absorption-line stellar kinematics (M32, NGC 4342), dynamics of gas disks (M87, NGC 4261), and velocities of discrete objects (MW, NGC 4258); while in Sample B all of the black hole masses were derived from stellar spectra obtained from the ground. This was circumstantial, but to us compelling, evidence that the Sample A galaxies were defining the true relation and that the Sample B black hole masses were systematically in error.

Fitting a regression line to $\log M_\bullet$ vs. $\log \sigma$ for the Sample A galaxies alone, we found

$$M_\bullet = 1.40 \times 10^8 M_\odot \left(\frac{\sigma_c}{200 \text{ km s}^{-1}} \right)^\alpha \quad (1)$$

with $\alpha = 4.80 \pm 0.5$ (Ferrarese & Merritt 2000). We defined the quantity σ_c to be the rms velocity of stars in an aperture of radius $r_e/8$ centered on the nucleus, with r_e the half-light radius of the bulge. This radius is large enough that the stellar velocities are expected to be affected at only the few percent level by the gravitational force from the black hole, but small enough that σ_c can easily be measured from the ground.

A striking feature of the $M_\bullet - \sigma$ relation is its negligible scatter. The reduced χ^2 of Sample A about the best-fit line of Eq. 1, taking into account measurement errors in both variables, is only 0.74, essentially a perfect fit. Such a tight correlation seemed almost too good to be true (and may in fact be a fluke resulting from the small sample size) but we felt we could not rule it out given the existence of other, similarly tight correlations in astronomy, e.g. the near-zero thickness of the elliptical galaxy fundamental plane.

In fact the scatter in the $M_\bullet - \sigma$ relation is so small that it is reasonable to use the relation to *predict* black hole masses, even in galaxies for which determinations of M_\bullet based on detailed modelling have previously been published. One can then ask, galaxy by galaxy, whether the observations on which the published estimate of M_\bullet was based were of sufficiently high quality to resolve the black hole's sphere of influence. Table 1 and Figure 2 show the results. Table 1 is a ranked list of the most secure black hole detections to date. The galaxies are listed in order of increasing $\text{FWHM}/2r_h$, i.e. the ratio of the size of the resolution element to twice the radius of influence of the black hole. In the case of HST observations, for which the PSF is undersampled, FWHM is the diameter of the FOS aperture or the width of the STIS slit. For ground-based observations, FWHM refers to the seeing disk. Figure 2 plots the same quantities for essentially all galaxies with published estimates of M_\bullet based on stellar or gas kinematics.

Not surprisingly, only the black holes in the Milky Way and in NGC 4258 have been observed at a resolution much greater than r_h . The Sample A galaxies of Ferrarese & Merritt (2000) also satisfy this condition, although sometimes marginally. By contrast, almost none of the ground based data resolved r_h , sometimes failing by more than a factor of 10.

The latter point is important, since precisely these data were used to define the canonical relation between black hole mass and bulge luminosity (Magorrian *et al.* 1998; Richstone *et al.* 1998; Ho 1999; Faber 1999) that has served as the basis for so many subsequent studies (e.g. Haehnelt, Natarajan & Rees 1998; Cattaneo, Haehnelt & Rees 1999; Salucci *et al.* 1999; Kauffmann & Haehnelt 2000; Merrifield, Forbes & Terlevich 2000). Figure 3 plots the likely error in the ground based mass estimates (defined as the ratio of the quoted mass, M_{fit} , to the mass implied by Eq. 1) as a function of the effective resolution $\text{FWHM}/2r_h$. The error is found to correlate strongly with the quality of the data. For the best-resolved of the Magorrian *et al.* candidates, $\text{FWHM}/2r_h \lesssim 1$, the average error in M_\bullet appears to be a factor of ~ 3 , rising roughly linearly with FWHM/r_h to values of $\sim 10^2$ for the most poorly-resolved candidates.

An important quantity is the mean ratio of black hole mass to bulge mass, $\langle M_\bullet/M_{\text{bulge}} \rangle$. Figure 4 compares the distribution of $M_{\text{fit}}/M_{\text{bulge}}$, the mass ratio computed by Magorrian *et al.* (1998), to the distribution obtained when M_{fit} is replaced by M_\bullet as computed from the $M_\bullet - \sigma$ relation. The mean value of $\langle M_\bullet/M_{\text{bulge}} \rangle$ drops from 1.7×10^{-2} to 2.5×10^{-3} , roughly an order of magnitude. The mean value of $\log_{10}(M_\bullet/M_{\text{bulge}})$ shifts downward by -0.7 corresponding to a factor ~ 5 in $M_\bullet/M_{\text{bulge}}$. The density of black holes in the local universe implied by the lower value of $\langle M_\bullet/M_{\text{bulge}} \rangle$ is $\rho_\bullet \sim 5 \times 10^5 M_\odot \text{Mpc}^{-3}$ (Merritt & Ferrarese 2001b), consistent with the value required to explain quasar luminosi-

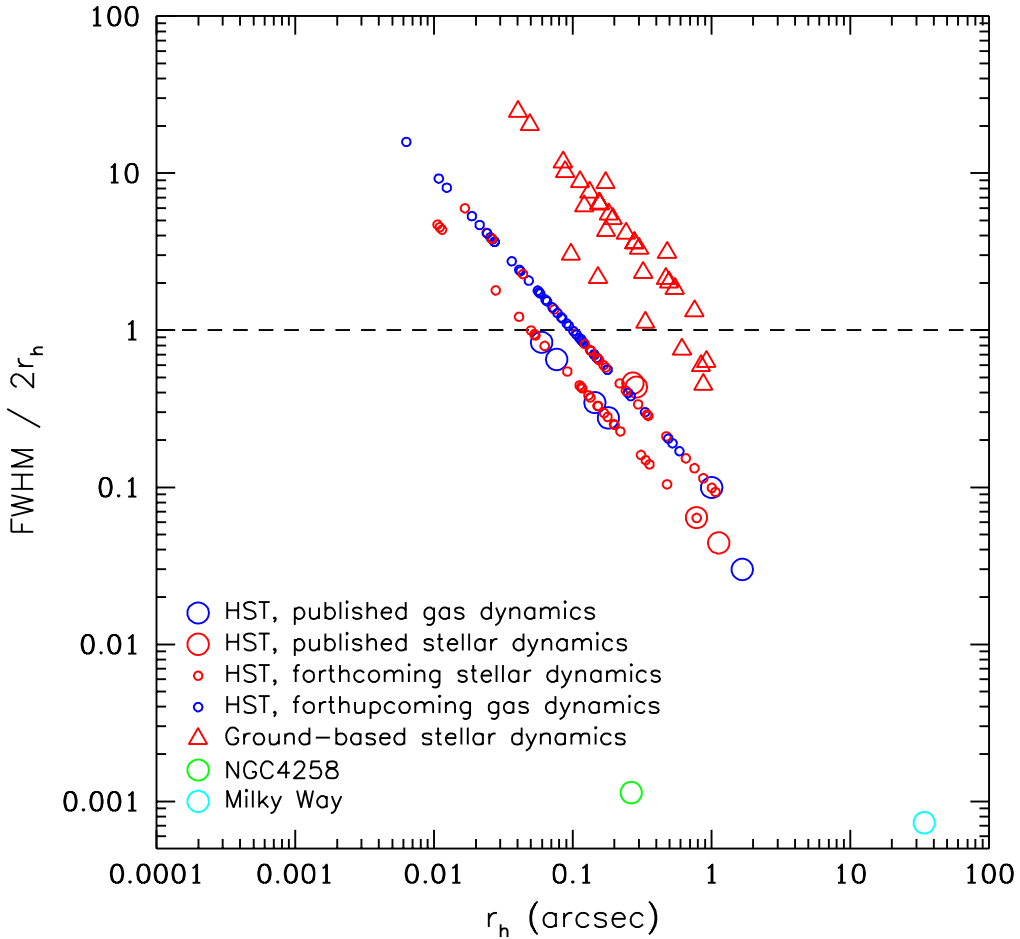


Figure 2. Detectability of black holes in galaxies for which dynamical mass determinations have been published or are planned. Horizontal axis is $r_h \equiv GM_\bullet/\sigma^2$, the black hole's radius of influence. M_\bullet is computed from the $M_\bullet - \sigma$ relation for all forthcoming and ground based observations. Vertical axis is the ratio of the observational resolution to twice r_h . Determination of M_\bullet is difficult when this ratio is $\gtrsim 1$, and mass determinations based on stellar dynamics (red symbols) can be difficult even when $\text{FWHM}/2r_h < 1$, for reasons discussed in the text.

Ranked Census of Supermassive Black Hole Detections ^{1,2}

| Galaxy | Type | Distance | M_{\bullet} | σ_c | FWHM/2 r_h | Reference |
|--|--|----------|----------------------------|--------------|----------------------------------|------------------------------------|
| Galaxies for which r_h has been resolved | | | | | | |
| MW | SbI-II | 0.008 | 0.0295 \pm 0.0035 | 100 \pm 20 | 7.3 $^{-4}$ | Genzel <i>et al.</i> 2000 |
| N4258 | SAB(s)bc | 7.2 | 0.390 \pm 0.034 | 138 \pm 18 | 1.1 $^{-3}$ | Miyoshi <i>et al.</i> 1995 |
| N4486 | E0pec | 16.7 | 35.7 \pm 10.2 | 345 \pm 45 | 0.03 | Macchetto <i>et al.</i> 1997 |
| N3115 | S0 $^{-}$ | 9.8 | 9.2 \pm 3.0 | 278 \pm 36 | 0.04 | Emsellem <i>et al.</i> 1999 |
| N221 | cE2 | 0.8 | 0.039 \pm 0.009 | 76 \pm 10 | 0.06 | Joseph <i>et al.</i> 2000 |
| N5128 | S0pec | 4.2 | 2.4 $^{+3.6}_{-7}$ | 145 \pm 25 | 0.10 | Marconi <i>et al.</i> 2001 |
| N4374 | E1 | 18.7 | 17 $^{+12}_{-6.7}$ | 286 \pm 37 | 0.10 | Bower <i>et al.</i> 1998 |
| N4697 | E6 | 11.9 | 1.7 $^{+0.2}_{-0.3}$ | 163 \pm 21 | 0.10 | Nuker group, unpubl. ³ |
| N4649 | E2 | 17.3 | 20.6 $^{+5.2}_{-10.2}$ | 331 \pm 43 | 0.10 | Nuker group, unpubl. ³ |
| N4261 | E2 | 33.0 | 5.4 $^{+1.2}_{-1.2}$ | 290 \pm 38 | 0.18 | Ferrarese <i>et al.</i> 1996 |
| M81 | SA(s)ab | 3.9 | 0.68 $^{+0.07}_{-0.13}$ | 174 \pm 17 | 0.19 | STIS IDT, unpubl. ³ |
| N4564 | E | 14.9 | 0.57 $^{+0.13}_{-0.17}$ | 153 \pm 20 | 0.33 | Nuker group, unpubl. ³ |
| I1459 | E3 | 30.3 | 4.6 \pm 2.8 | 312 \pm 41 | 0.35 | Verdoes Kleijn <i>et al.</i> 2000 |
| N5845 | E* | 28.5 | 2.9 $^{+1.7}_{-2.7}$ | 275 \pm 36 | 0.40 | Nuker group, unpubl. ³ |
| N3379 | E1 | 10.8 | 1.35 \pm 0.73 | 201 \pm 26 | 0.44 | Gebhardt <i>et al.</i> 2000a |
| N3245 | SB(s)b | 20.9 | 2.1 \pm 0.5 | 211 \pm 19 | 0.48 | Barth <i>et al.</i> 2001 |
| N4342 | S0 $^{-}$ | 16.7 | 3.3 $^{+1.9}_{-1.1}$ | 261 \pm 34 | 0.56 | Cretton & van den Bosch 1999 |
| N7052 | E | 66.1 | 3.7 $^{+2.6}_{-1.5}$ | 261 \pm 34 | 0.66 | van der Marel & van den Bosch 1998 |
| N4473 | E5 | 16.1 | 0.8 $^{+1.0}_{-0.4}$ | 188 \pm 25 | 0.77 | Nuker group, unpubl. ³ |
| N6251 | E | 104 | 5.9 \pm 2.0 | 297 \pm 39 | 0.84 | Ferrarese & Ford 1999 |
| N2787 | SB(r)0+ | 7.5 | 0.41 $^{+0.04}_{-0.05}$ | 210 \pm 23 | 0.87 | Sarzi <i>et al.</i> 2001 |
| N3608 | E2 | 23.6 | 1.1 $^{+1.4}_{-0.3}$ | 206 \pm 27 | 0.98 | Nuker group, unpubl. ³ |
| Galaxies for which r_h has not been resolved | | | | | | |
| N3384 | SB(s)0 $^{-}$ | 11.9 | 0.14 $^{+0.05}_{-0.04}$ | 151 \pm 20 | 1.0 | Nuker group, unpubl. ³ |
| N4742 | E4 | 15.5 | 0.14 $^{+0.04}_{-0.05}$ | 93 \pm 10 | 1.0 | STIS IDT, unpubl. ³ |
| N1023 | S0 | 10.7 | 0.44 \pm 0.06 | 201 \pm 14 | 1.1 | STIS IDT, unpubl. ³ |
| N4291 | E | 26.9 | 1.9 $^{+1.3}_{-1.1}$ | 269 \pm 35 | 1.1 | Nuker group, unpubl. ³ |
| N7457 | SA(rs)0 $^{-}$ | 13.5 | 0.036 $^{+0.009}_{-0.011}$ | 73 \pm 10 | 1.1 | Nuker group, unpubl. ³ |
| N821 | E6 | 24.7 | 0.39 $^{+0.17}_{-0.15}$ | 196 \pm 26 | 1.3 | Nuker group, unpubl. ³ |
| N3377 | E5+ | 11.6 | 1.10 $^{+1.4}_{-0.5}$ | 131 \pm 17 | 1.3 | Nuker group, unpubl. ³ |
| N2778 | E | 23.3 | 0.13 $^{+0.16}_{-0.08}$ | 171 \pm 22 | 2.8 | Nuker group, unpubl. ³ |
| Galaxies in which dynamical studies are inconclusive | | | | | | |
| N224 | Double nucleus, system not in dynamical equilibrium. | | | | Bacon <i>et al.</i> 2001 | |
| N598 | Data imply upper limit only, $M_{\bullet} \lesssim 10^3 M_{\odot}$. | | | | Merritt, Ferrarese & Joseph 2001 | |
| N1068 | Velocity curve is sub-Keplerian. | | | | Greenhill <i>et al.</i> 1996 | |
| N3079 | Masers do not trace a clear rotation curve. | | | | Trotter <i>et al.</i> 1998 | |
| N4459 | Data do not allow unconstrained fits. | | | | Sarzi <i>et al.</i> 2001 | |
| N4486B | Double nucleus, system not in dynamical equilibrium. | | | | STIS IDT, unpubl. ² | |
| N4945 | Asymmetric velocity curve; velocity is sub-Keplerian. | | | | Greenhill <i>et al.</i> 1997 | |

¹Type is revised Hubble type. Black hole masses are in 10^8 solar masses, velocity dispersions are in km s^{-1} , and distances are in Mpc. σ_c is the aperture-corrected velocity dispersion defined by Ferrarese & Merritt (2000). $r_h = GM_{\bullet}/\sigma_c^2$, with M_{\bullet} the value in column 4. References in column 7 are to the papers in which the dynamical analysis leading to the mass estimate were published.

²For the reasons outlined in the text, the masses from Magorrian *et al.* (1998) are omitted from this tabulation. This includes NGC 4594, which was included in Kormendy & Gebhardt (2001).

³Preliminary masses tabulated in Kormendy & Gebhardt (2001). Data and modelling for these mass estimates are not yet available.

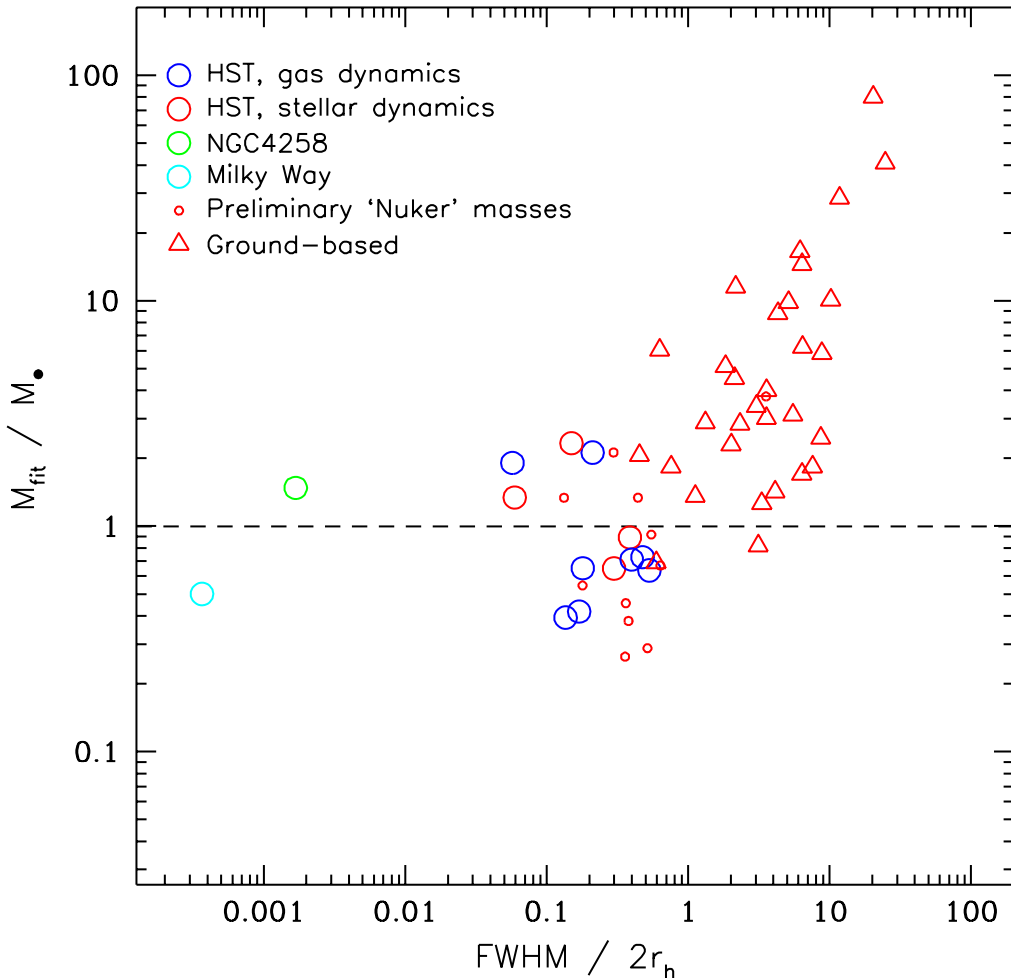


Figure 3. “Error” in published black hole masses, defined as the ratio of the published mass estimate M_{fit} to the value M_{\bullet} inferred from the $M_{\bullet} - \sigma$ relation, as a function of the effective resolution of the data from which the mass estimate was derived. The error increases roughly inversely with resolution for $\text{FWHM}/2r_h \gtrsim 1$. Most of the ground based detections are in this regime.

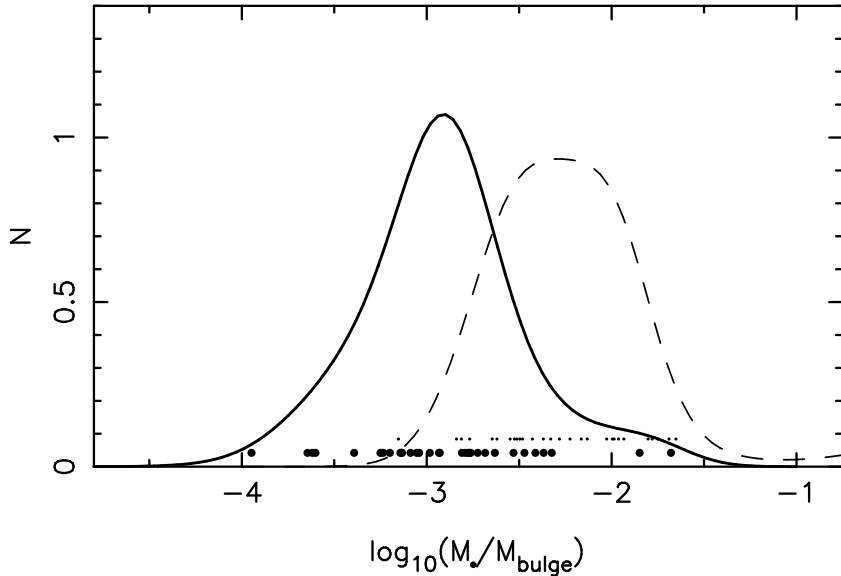


Figure 4. Frequency function of black-hole-to-bulge mass ratios (adapted from Merritt & Ferrarese 2001a). Dashed curve is the “Magorrian relation” (Magorrian *et al.* 1998) based on black hole masses derived from ground-based kinematics and two-integral modelling. Solid curve is the frequency function obtained when black hole masses are computed instead from the $M_{\bullet} - \sigma$ relation.

ties assuming a standard accretion efficiency of 10% (Chokshi & Turner 1992; Salucci *et al.* 1999; Barger *et al.* 2001).

2.2. Pitfalls of Stellar Dynamical Mass Estimation

Why were most of the stellar dynamical mass estimates so poor; why were they almost always over-estimates; and what lessons do past mistakes have for the future? The answer to the first question is simple in retrospect. Figure 5 shows how the signal of the black hole – a sudden rise in the rms stellar velocities at a distance of $\sim r_h \equiv GM_{\bullet}/\sigma^2$ from the black hole – is degraded by seeing. For $\text{FWHM}/2r_h \gtrsim 2$, the signal is so small as to be almost unrecoverable except with data of exceedingly high S/N . Most of the ground based observations fall into this regime (Figure 2). In fact the situation is even worse than Figure 5 suggests, since for $\text{FWHM} \gtrsim r_h$, the rise in $\sigma(R)$ will be measured by only a single data point. This is the case for many of the galaxies that are listed as “resolved” in Table 1 (e.g. NGC 3379, Gebhardt *et al.* 2000a).

A short digression is in order at this point. Data taken from the ground often show an impressive central spike in the velocity dispersion profile; examples are NGC 4594 (Kormendy *et al.* 1996b) and NGC 4486b (Kormendy *et al.* 1997). However such features are due in part to blending of light from two sides of the nucleus where the rotational velocity has opposite signs and would be almost as impressive even if the black hole were not present. This point was first emphasized by Tonry (1984) in the context of his ground based M32 observations. As he showed, the velocity dispersion spike in M32 as observed

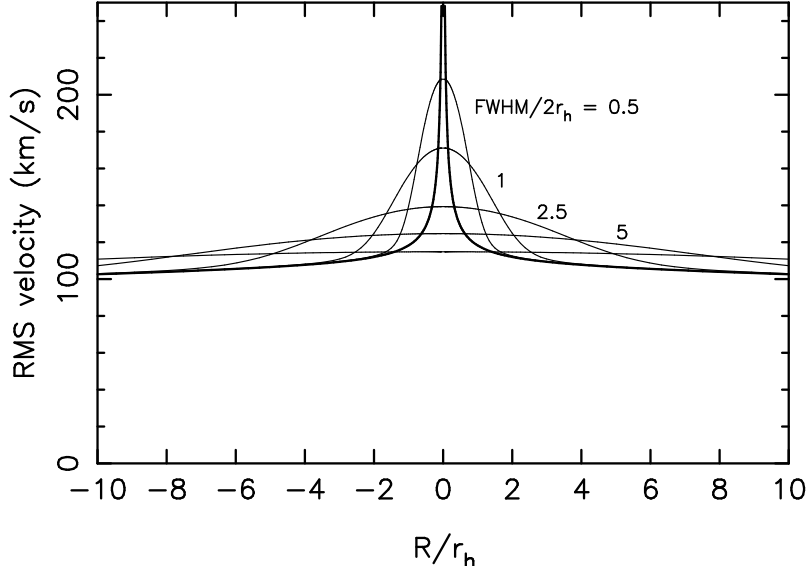


Figure 5. Degradation due to seeing of the velocity dispersion spike produced by a black hole in a hot (nonrotating) stellar system. Heavy line is the profile unaffected by seeing; R is the projected distance from the black hole and $r_h = GM_\bullet/\sigma^2$. When $\text{FWHM}/2r_h$ exceeds ~ 2 , the velocity dispersion spike is so degraded as to be almost unrecoverable. Most ground based observations fall into this regime (Fig. 2).

at $\sim 1''$ resolution is consistent with rotational broadening and does not require any increase in the *intrinsic* velocity dispersion near the center.

Why should poor data lead preferentially to overestimates of M_\bullet , rather than random errors? There are two reasons. First, as pointed out by van der Marel (1997), much of the model-fitting prior to 1999 was carried out using isotropic spherical models or their axisymmetric analogs, the so-called “two-integral” (2I) models. Such models predict a velocity dispersion profile that gently *falls* as one moves inward, for two reasons: non-isothermal cores, i.e. $\rho \sim r^{-\gamma}$ with $\gamma \neq \{0, 2\}$, generically have central minima in the rms velocity (e.g. Dehnen 1993); and, when flattened, the 2I axisymmetric models become dominated by nearly circular orbits (in order to maintain isotropy in the meridional plane) further reducing the predicted velocities near the center. Figure 6 illustrates these effects for a set of axisymmetric 2I models with $\gamma = 1.5$. Real galaxies almost always exhibit a monotonic rise in v_{rms} . Adding a central point mass can correct this deficiency of the models, but only an unphysically large value of M_{fit} will affect the stellar motions at large enough radii, $r \gtrsim 0.1r_e$, to do the trick. This is probably the explanation for the factor ~ 3 mean error in M_\bullet derived from the best ground based data (Figure 3).

The much larger values of M_{fit}/M_\bullet associated with the more distant galaxies in Figure 3 are probably attributable to a different factor. When the data contain no useful information about the black hole mass, only values of M_{fit} that are much larger than the true mass will significantly affect the χ^2 of the model fits.

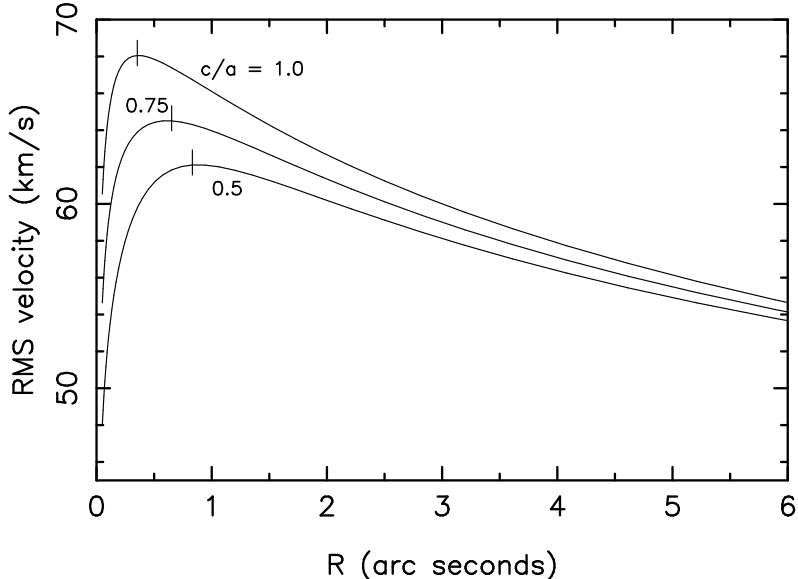


Figure 6. Velocity dispersion profiles of the “two-integral” (2I) models that were used as templates for estimating black hole masses in many of the stellar kinematical studies (e.g. Magorrian *et al.* 1998). Model flattening is indicated as c/a ; there are no central black holes. Ticks mark the point R_{max} of maximum velocity; R_{max} moves outward as the flattening is increased.

The only black holes that can be “seen” in such data are excessively massive ones.

Can these problems be overcome by abandoning 2I models in favor of more general, three-integral (3I) models? The answer, surprisingly, is “no”: making the modelling algorithm more flexible (without also increasing the amount or quality of the data) has the effect of *weakening* the constraints on M_\bullet . The reason is illustrated in Figure 7. The rms velocities in 2I models are uniquely determined by the assumed potential, i.e. by M_{fit} and M/L , the mass-to-light ratio assumed for the stars. This means that the models are highly *over-constrained* by the data – there are far more observational constraints (velocities) than adjustable parameters (M_{fit}, M_\bullet), hence one expects to find a unique set of values for M_{fit} and M/L that come closest to reproducing the data. This is the usual case in problems of statistical estimation and it implies a well-behaved set of χ^2 contours with a unique minimum.

When the same data are modeled using the more general distribution of orbits available in a 3I model, the problem becomes *under-constrained*: now one has the freedom to adjust the phase-space distribution function in order to compensate for changes in M_{fit} and M/L , so as to leave the goodness-of-fit precisely unchanged. The result is a plateau in χ^2 (Figure 7), the width of which depends in a complicated way on the ratio of observational constraints to number of orbits or phase-space cells in the modelling algorithm (Merritt 1994). Thus, 3I modelling of the ground-based data would only show that the range of possible values of M_{fit} includes, but is not limited to, the values found using the

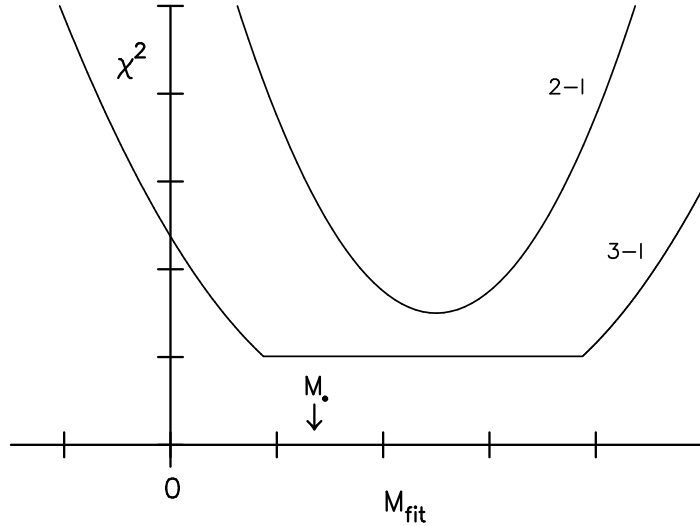


Figure 7. Schematic comparison of two-integral (2I) and three-integral (3I) modelling of stellar kinematical data; M_{fit} is the estimated black hole mass. 2I models predict a unique rms velocity field given an assumed mass distribution; in 3I models, the extra freedom associated with a more general distribution of orbits allows one to compensate for changes in M_{fit} in such a way as to leave the goodness of fit to the data precisely unchanged.

2I models; it would not generate more precise estimates of M_{\bullet} unless the data quality were also increased.

The greater difficulty of interpreting results from 3I modelling has not been widely appreciated; few authors make a distinction between “indeterminacy” in M_{\bullet} (the width of the constant- χ^2 plateau in Figure 7) and “uncertainty” (the additional range in M_{\bullet} allowed by measurement errors), or look carefully at how their confidence range depends on the number of orbits used. We illustrate these difficulties by looking at two recently published studies based on high quality, stellar kinematical data.

1. *NGC 3379* (Gebhardt *et al.* 2000a): The prima-facie evidence for a central mass concentration in this galaxy consists of a single data point, the innermost velocity dispersion as measured by HST/FOS; the rotation curve exhibits no central rise, in fact it drops monotonically toward the center. Goodness-of-fit contours generated from 3I models show the expected plateau (Fig. 7 of Gebhardt *et al.*), extending from $\sim 10^6 M_{\odot}$ to $\sim 3 \times 10^8 M_{\odot}$. In fact a model with $M_{\bullet} = 0$ fits the data just as well: the authors state that “the difference between the no-black hole and black hole models is so subtle” as to be almost indiscernable (cf. their Fig. 11). Gebhardt *et al.* nevertheless argue for $M_{\bullet} > 0$ based on the poorly-determined wings of stellar velocity distribution measured within the central FOS resolution element. In view of the fact that this velocity distribution exhibits a puzzling unexplained asymmetry (their Fig. 4), the stellar dynamical case for a black hole in this galaxy should probably be considered marginal.

2. *NGC 4342* (Cretton and van den Bosch 1999): The evidence for a central mass concentration is again limited to a single data point, the central FOS velocity dispersion. Cretton & van den Bosch find that a black-hole-free model provides “fits to the actual data [that] look almost indistinguishable from that of Model B” (a model with $M_{\text{fit}} = 3.6 \times 10^8 M_{\odot}$). Their χ^2 contours (their Fig. 7) nevertheless seem to show a preferred black hole mass; however they note that χ^2 is dominated by the data at radii $R \gtrsim 5''$, far outside of the radius of influence of the black hole. The probable culprit here is the modest number of orbits (1400, compared with ~ 250 constraints) in their 3I solutions. Outer data points are always the most difficult to fit when modelling via a finite orbit library since only a fraction of the orbits extend to large radii; this is clear in their fits (cf. their Fig. 8) which become progressively worse at large radii.

We emphasize that both of these modelling studies were based on high-quality data, with $\text{FWHM}/2r_h \approx 0.4$ (NGC 3379) and 0.6 (NGC 4342) (Table 1). Nevertheless, the extreme freedom associated with 3I models permits a wide range of black hole masses to be fit to the velocity data in both galaxies. As Figure 2 shows, most of the galaxies in the ongoing HST/STIS survey of galactic nuclei will be observed at even lower effective resolutions; hence we predict that the black hole masses in many of these galaxies will turn out to be consistent with zero and that the range of allowed masses will usually be large. (To be fair, we note that these observations were planned at a time when $\langle M_{\bullet}/M_{\text{bulge}} \rangle$ was believed to be much larger than it is now.) We therefore urge caution when interpreting results like Kormendy & Gebhardt’s (2001) recent compilation of black hole masses derived from unpublished 3I modelling.

3. Supermassive Black Holes in Active Galactic Nuclei

The techniques that allow us to detect supermassive black holes in quiescent galaxies are rarely applicable to the hosts of bright AGNs. In the Seyfert 1 galaxies and in the handful of QSOs that are close enough that the black hole’s sphere of influence has some chance of being resolved, the presence of the bright non-thermal nucleus (e.g. Malkan, Gorjian & Tam 1998) severely dilutes the very features which are necessary for dynamical studies. The only bright AGN in which a supermassive black hole has been detected by spatially-resolved kinematics is the nearby (Herrnstein *et al.* 1999; Newman *et al.* 2000) Seyfert 2 galaxy NGC 4258, which is blessed by the presence of an orderly water maser disk (Watson & Wallin 1994; Greenhill *et al.* 1995; Miyoshi *et al.* 1995). The radius of influence of the black hole at its center, $\sim 0''.15$, can barely be resolved by HST but can be fully sampled by the VLBA at 22.2 GHz. Unfortunately, water masers are rare and of the handful that are known, only in NGC 4258 are the maser clouds distributed in a simple geometrical configuration that exhibits clear Keplerian motion around the central source (Braatz *et al.* 1996; Greenhill *et al.* 1996, 1997; Greenhill, Moran & Herrnstein 1997; Trotter *et al.* 1998). Black hole demographics in AGNs must therefore proceed through alternative techniques.

Dynamical modeling of the broad emission line region (BLR) constitutes a viable alternative to spatially-resolved kinematical studies. According to the standard model, the BLR consists of many (10^{7-8} , Arav *et al.* 1997, 1998; Di-

etrich *et al.* 1999), small, dense ($N_e \sim 10^{9-11} \text{ cm}^{-3}$), cold ($T_e \sim 2 \times 10^4 \text{ K}$) photoionized clouds (Ferland *et al.* 1992), localized within a volume of a few light days to several tens of light weeks in diameter around the central ionization source (but see also Smith & Raine 1985, 1988; Pelletier & Pudritz 1992; Murray *et al.* 1995; Murray & Chiang 1997; Collin-Souffrin *et al.* 1988). As such, the BLR is, and will likely remain, spatially unresolved. In the presence of a variable non-thermal nuclear continuum, however, the responsivity-weighted radius R_{BLR} of the BLR is measured by the light-travel time delay between emission and continuum variations (Blandford & McKee 1982; Peterson 1993; Netzer & Peterson 1997; Koratkar & Gaskell 1991). If the BLR is gravitationally bound, the central mass is given by the virial theorem as $M_{\text{virial}} = v_{BLR}^2 R_{BLR}/G$, where the FWHM of the emission lines (generally H β) is taken as being representative of the rms velocity v_{BLR} , once assumptions are made about the BLR geometry. In a few cases, independent measurements of R_{BLR} and v_{BLR} have been derived from different emission lines: it is found that the two quantities define a “virial relation” in the sense $v_{BLR} \sim r^{-1/2}$ (Koratkar & Gaskell 1991; Wandel, Peterson & Malkan 1999; Peterson & Wandel 2000), suggesting a simple picture of a stratified BLR in Keplerian motion.

On the downside, mapping the BLR response to continuum variations requires many ($\sim 10^{1-2}$) repeated observations taken at closely spaced time intervals, $\Delta t \lesssim 0.1 R_{BLR}/c$. Moreover, the observations can be translated into black hole masses only if a series of reasonable, but untested, assumptions are made regarding the geometry, stability and velocity structure of the BLR, the radial emissivity function of the gas, and the geometry and location (relative to the BLR) of the ionizing continuum source. If a wrong assumption is made, systematic errors of a factor ~ 3 can result (Krolik 2001). The uncertainties surrounding reverberation mapping has made the derived black hole masses an easy target for critics (e.g. Richstone *et al.* 1998; Ho *et al.* 1999). On the other hand, because the BLR gas samples a spatial region very near to the black hole, there is almost no possibility of making the much larger errors in M_{\bullet} that have plagued the ground-based stellar kinematical studies (Magorrian *et al.* 1998). Thanks to the efforts of international collaborations, reverberation mapping masses are now available for 17 Seyfert 1 galaxies and 19 QSOs (Wandel, Peterson & Malkan 1999; Kaspi *et al.* 2000).

Taken at face value, reverberation mapping radii are found to correlate with the non-thermal optical luminosity of the nuclear source. While the exact functional form of the dependence is debated (Koratkar & Gaskell 1991; Kaspi *et al.* 1996, 2000; Wandel, Peterson & Malkan 1999), the $R_{BLR} - L$ relation can potentially provide an inexpensive way of bypassing reverberation mapping measurements on the way to determining black hole masses.

3.1. AGN Black Hole Demographics from the $M_{\bullet} - M_{\text{bulge}}$ Relation

With one exception (Ferrarese *et al.* 2001), black hole demographic studies for AGNs have been based on the $M_{\bullet} - M_B$, rather than on the $M_{\bullet} - \sigma$, relation for the simple reason that few accurate σ measurements exist in AGN hosts (e.g. Nelson & Whittle 1995). L_{bulge} , on the other hand, is more easily measured than σ (though not necessarily more *accurately* measured, as discussed below). The modest sample of AGNs with reverberation mapping black hole masses is

often augmented using masses derived from the $R_{BLR} - L$ relation (Wandel 1999; Laor 1998, 2000; McLure & Dunlop 2000). For a sample of 14 PG quasars, Laor (1998) reported reasonable agreement with the $M_\bullet - M_B$ relation derived by Magorrian *et al.* (1998) for quiescent galaxies, finding $\langle M_\bullet/M_{\text{bulge}} \rangle = 0.006$. Seyfert 1 galaxies define a significantly different correlation according to Wandel (1999): $\langle M_\bullet/M_{\text{bulge}} \rangle = 0.0003$. Most recently, McLure & Dunlop (2000) have reanalyzed the QSO sample of Laor and the Seyfert sample of Wandel (the first augmented with almost as many new objects and both with new spectroscopic and/or photometric data for the existing objects). McLure & Dunlop split the difference of the two earlier studies by obtaining $\langle M_\bullet/M_{\text{bulge}} \rangle = 0.0025$. They find no statistical difference between Seyfert 1s and QSOs.

The different conclusions reached by these authors can be traced to a number of factors.

- Bulge magnitudes are at the heart of the problem for the Seyfert sample (McLure & Dunlop 2000; Laor 2001). Wandel used luminosities derived (by Whittle *et al.* 1992) using the Simien & de Vaucouleurs (1986) empirical correlation between galaxy type and bulge/disk ratio. HST images allowed McLure & Dunlop to perform a proper disk/bulge decomposition, which produces bulges 1–3.5 magnitudes fainter than assumed by Wandel (1999), hence larger $M_\bullet/M_{\text{bulge}}$.
- Overestimated black hole masses seem to be responsible for the large $\langle M_\bullet/M_{\text{bulge}} \rangle$ measured by Laor. Here, the bolometric non-thermal nuclear luminosity used in estimating R_{BLR} from the $R_{BLR} - L$ relation is a factor ~ 3 larger in Laor than in McLure & Dunlop (for the same cosmology). Everything else being equal, this leads to a factor ~ 2 increase in the black hole masses. It is unclear which luminosities are more correct; however it seems that the McLure & Dunlop values are to be preferred for the following reason. The $R_{BLR} - L$ relation is defined using monochromatic luminosity (at 5100 Å in Kaspi *et al.* 2000, and 4800 Å in Kaspi *et al.* 1996). This can be transformed to a bolometric luminosity by assuming a power law of given spectral index for the nuclear spectrum. McLure & Dunlop used monochromatic luminosities applied to the Kaspi *et al.* (2000) relation, while Laor started from bolometric luminosities (from Neugebauer *et al.* 1987), applied a constant bolometric correction, and then used the Kaspi *et al.* (1996) relation. The more direct route used by McLure & Dunlop (which bypasses the need for a bolometric correction) seems to be preferable.

We have recomputed the data from the Wandel (1999) and McLure & Dunlop (2000) studies under a uniform set of assumptions, as follows:

- $H_0 = 75 \text{ km s}^{-1} \text{ Mpc}^{-1}$. While black hole masses are independent of cosmology, bulge magnitudes are not. For nearby quiescent galaxies with dynamically detected black holes, distances are estimated directly, mainly using the surface brightness fluctuation method (SBF). SBF distances to galaxies in the (mostly) unperturbed Hubble flow lead to $H_0 = 70 - 77 \text{ km s}^{-1} \text{ Mpc}^{-1}$ (Ferrarese *et al.* 2000; Tonry *et al.* 2001); $H_0 = 75 \text{ km}$

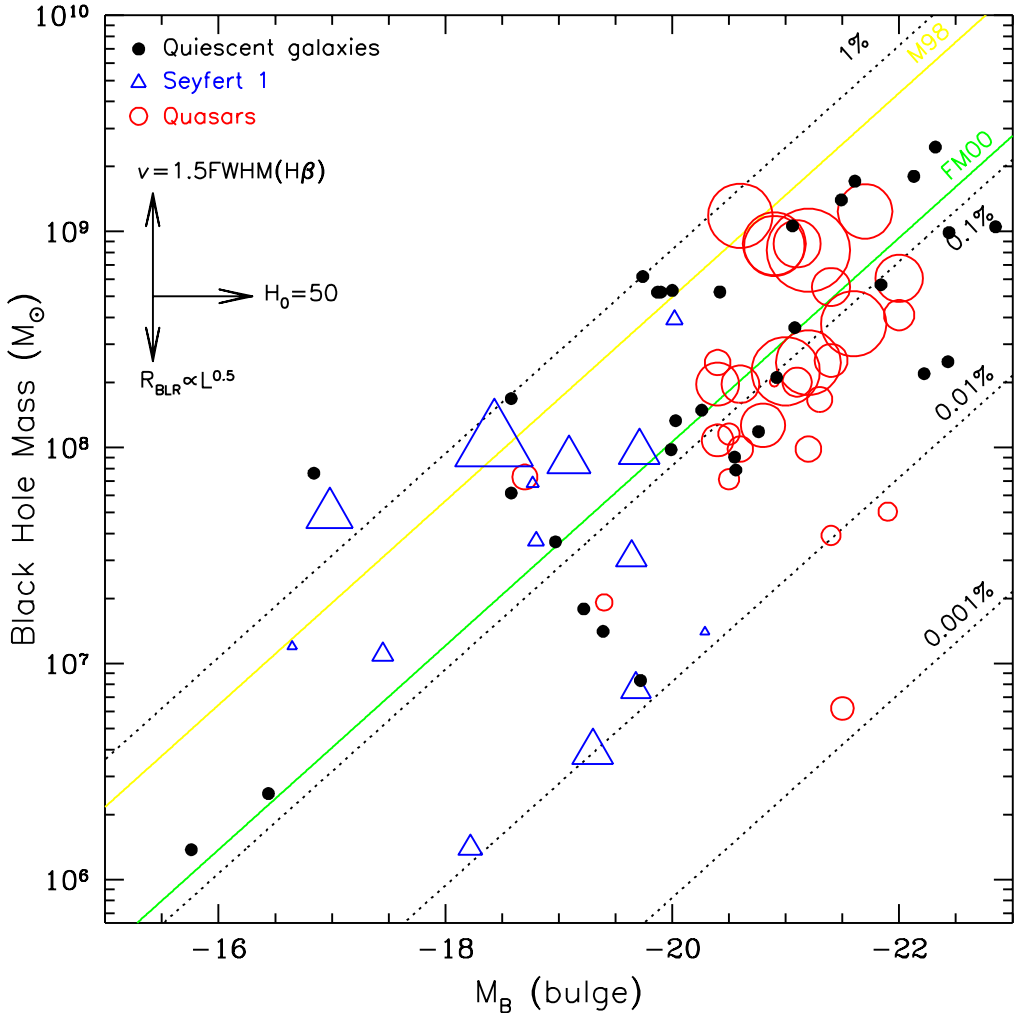


Figure 8. The $M_{\bullet}/M_{\text{bulge}}$ relation for quiescent galaxies (solid black dots, with best fit given by the green line), Seyfert 1 galaxies (blue triangles) and nearby QSOs (red circles). The data are taken from Ferrarese & Merritt (2000), McLure & Dunlop (2000) and Wandel, Peterson & Malkan (1999). When necessary, bulge magnitudes are converted to Johnsons B by adopting $V - R = 0.59$ and $B - V = 0.93$. The size of the symbols for the AGNs is proportional to the $\text{H}\beta$ FWHM: the nominal distinction between narrow and broad line AGNs occurs at the FWHM represented by the symbol size used in the legend. The yellow line represents the best fit to the nearby quiescent galaxies derived by Magorrian *et al.* (1998); the green line is fit to the black hole masses from Merritt & Ferrarese (2001a) (shown as filled circles). The dotted black lines are the loci for which the black hole mass is a fixed percentage of the bulge mass. The arrows in the upper left corner represent the change in M_{\bullet} or M_{bulge} produced under assumptions different from the ones detailed in the text.

$\text{s}^{-1} \text{ Mpc}^{-1}$ therefore gives distances, for the distant QSOs and Seyfert 1s, on the same distance scale used for the nearby quiescent galaxies. Using $H_0 = 50 \text{ km s}^{-1} \text{ Mpc}^{-1}$ instead, as in McLure and Dunlop, would inflate AGN bulge luminosities by a factor 2.25 (and the masses by a factor ~ 2.7 ; see below).

- $R_{BLR} = 32.9(\lambda L_{5100}/10^{44} \text{ ergs s}^{-1})^{0.7}$ light days (Kaspi *et al.* 2000). While it is likely that the slope of this correlation will be refined once accurate estimates of R_{BLR} are obtained at low and high luminosities, this is currently the best estimate of the functional form of the $R_{BLR} - L$ relation. Because all QSOs have higher luminosities than the objects that define the $R_{BLR} - L$ relation, adopting $R_{BLR} \propto (\lambda L_{5100})^{0.5}$ (e.g. Kaspi *et al.* 1996) would lead to estimates of R_{BLR} and M_\bullet that are 1.5 to 3 times smaller respectively.
- $v_{BLR} = \sqrt{3}/2 \text{ FWHM}(\text{H}\beta)$, i.e. the BLR is spherical and characterized by an isotropic velocity distribution. This differs from the assumption made by McLure & Dunlop that the BLR is a thin, rotation-dominated disk, i.e. $v = 1.5 \text{ FWHM}(\text{H}\beta)$, which predicts velocities 1.7 times larger and black holes masses three times greater.
- $M/L \propto L^{0.18}$ (Magorrian *et al.* 1998). This is the relation defined by the local sample of quiescent galaxies, for which Merritt & Ferrarese (2001a) derived $M_\bullet/M_{\text{bulge}} = 0.13\%$. Fundamental plane studies (Jorgensen, Franx & Kjaergaard 1996) point to a steeper dependence: $M/L \propto L^{0.34}$. Accounting for the proper normalization, and given the range in luminosity spanned by the QSOs and Seyfert 1 galaxies, using the latter relation would increase *all* inferred $M_\bullet/M_{\text{bulge}}$ ratios by a factor ~ 2.5 .

The results are shown in Figure 8. We draw the following conclusions.

1. The Seyfert, QSO and quiescent galaxy samples are largely consistent. A simple least-squares fit gives $\langle M_\bullet/M_{\text{bulge}} \rangle = 0.09\%$ (QSOs) and 0.12% (Seyferts), compared with $\langle M_\bullet/M_{\text{bulge}} \rangle = 0.13\%$ for quiescent galaxies (Merritt & Ferrarese 2001a). We further note that the disk/bulge decompositions for two of the objects with low $M_\bullet/M_{\text{bulge}}$, $0.001\% - 0.001\%$, are deemed of lower quality (McLure & Dunlop 2000). Thus it does not appear to be the case, as suggested by Richstone *et al.* (1998) and Ho (1999), that supermassive black holes in AGN are undermassive relative to their counterparts in quiescent galaxies. In fact, assuming a flattened BLR geometry would further increase the AGN masses.
2. $\langle M_\bullet/M_{\text{bulge}} \rangle$ in AGNs is lower, by a factor ~ 6 , than predicted by the Magorrian (1998) relation. This is further evidence that the mass estimates derived from ground-based kinematics were systematically in error.
3. In view of recent claims, it is interesting to ask whether narrow line Seyfert 1s and QSOs (Osterbrock & Pogge 1985) contain smaller black holes compared with the rest of the AGN sample (Véron-Cetty, Véron & Goncalves 2001 and references therein; Mathur *et al.* 2001). The size of the symbols

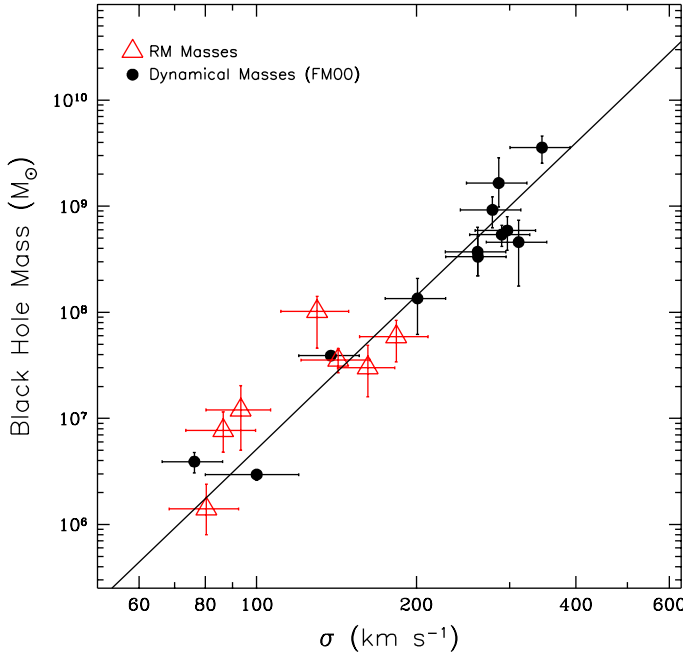


Figure 9. Black hole mass versus central velocity dispersion for seven reverberation-mapped AGNs with accurately measured velocity dispersions, compared with the nearby quiescent galaxy sample of Ferrarese & Merritt (2000) (plot adapted from Ferrarese *et al.* 2001).

in Figure 8 is proportional to the FWHM of the $H\beta$ line: the boundary between regular and narrow line objects corresponds to the size used in the figure legend. No correlation between line width and $M_\bullet/M_{\text{bulge}}$ is readily apparent for the Seyferts, while a hint might be present for the QSOs. On the other hand, bulge/disk decompositions are less accurate for most of the narrow line QSOs, and it is possible that bulge luminosities in these objects have been overestimated.

4. The large uncertainties in the data, and the large intrinsic scatter in the $M_\bullet - M_B$ relation, make it very difficult to test whether the relation between M_\bullet and M_{bulge} is linear. However, an ordinary least square fit to the data produces slopes consistent, at the 1σ level, with a linear relation for both the QSO and Seyfert 1 samples (cf Laor 2001).

3.2. AGN Black Hole Demographics from the $M_\bullet - \sigma$ Relation.

Because of its large intrinsic scatter, there is little more that can be learned about black hole demographics from the $M_\bullet - M_B$ relation. An alternative route is suggested by the $M_\bullet - \sigma$ relation for quiescent galaxies, which exhibits much less scatter. Very few accurate measurements of σ are available in AGNs, due to the difficulty of separating the bright nucleus from the faint underlying stellar population. The first program to map AGNs onto the $M_\bullet - \sigma$ relation was undertaken by Ferrarese *et al.* (2001). Velocity dispersions in the bulges of six galaxies with reverberation mapping masses were obtained, thus producing

the first sample of AGNs for which both the black hole mass and the stellar velocity dispersion are accurately known (with formal uncertainties of 30% and 15% respectively).

Figure 9 shows the relation between black hole mass and bulge velocity dispersion for the six reverberation-mapped AGNs observed by Ferrarese *et al.* (2001), plus an additional object with a high-quality σ from the literature (Nelson & Whittle 1995). The quiescent galaxies (from Ferrarese & Merritt 2000) are shown by the black dots. The consistency between black hole masses in active and quiescent galaxies is even more striking here than in the $M_\bullet - M_{\text{bulge}}$ plot. The only noticeable difference between the two samples is a slightly greater scatter in the reverberation mapping masses (in spite of similar, formal error bars). Narrow line Seyfert 1 galaxies do not stand out in any way from the rest of the AGN sample.

We conclude that there is no longer any *prima facie* reason to believe that reverberation-based masses are less reliable than those based on the kinematics of stars or gas disks. This is important since the resolution of stellar kinematical studies will remain fixed at $\sim 0''.1$ for the foreseeable future, whereas reverberation mapping samples a region which is *per se* unresolvable and is the only technique that can yield accurate masses for very small ($\lesssim 10^6 M_\odot$) or very distant black holes.

4. Recent and Future Refinements of the $M_\bullet - \sigma$ Relation

4.1. M33 – No Supermassive Black Hole?

The smallest nuclear black holes whose masses have been securely established are in the Milky Way and M32, both of which have $M_\bullet \approx 3 \times 10^6 M_\odot$ (Table 1). How small can supermassive black holes be? Some formation scenarios (e.g. Haenhelt, Natarajan & Rees 1998) naturally predict a lower limit of $\sim 10^6 M_\odot$. Black holes of lower mass have been hypothesized to hide within off-nuclear “Ultra Luminous X-Ray Sources” (ULXs: Matsumoto *et al.* 2001; Fabbiano *et al.* 2001), but their formation mechanisms are envisioned to be completely different (e.g. Miller & Hamilton 2001). Observationally, a black hole with $M_\bullet \leq 10^6 M_\odot$ could only be resolved in a very nearby galaxy. An obvious candidate is the Local Group late type spiral M33: the absence of an obvious bulge, and the low central stellar velocity dispersion ($\sigma \sim 20 \text{ km s}^{-1}$, Kormendy & McLure 1993) both argue for a very small black hole. According to the $M_\bullet - \sigma$ relation (Eq. 2), $M_\bullet \sim 3 \times 10^3 M_\odot$, but a range of at least $1 - 10 \times 10^3 M_\odot$ is allowed given the uncertainties in the slope of the relation.

We show in Figure 10 the rotation curve and velocity dispersion profile of the M33 nucleus obtained from HST/STIS data (Merritt, Ferrarese & Joseph 2001). There is an unambiguous *decrease* in the stellar velocity dispersion toward the center of the nucleus: the central value is $24 \pm 3 \text{ km s}^{-1}$, significantly lower than its value of $\sim 35 \pm 5 \text{ km s}^{-1}$ at $\pm 0.3'' \approx 1.2 \text{ pc}$. The rotation curve is consistent with solid-body rotation. A dynamical analysis gives an upper limit to the central mass of $\sim 3 \times 10^3 M_\odot$. While this is tantalizingly similar to the masses inferred for ULXs (Matsumoto *et al.* 2001; Fabbiano, Zezas & Murray 2001), the consistency of this upper limit with the $M_\bullet - \sigma$ relation (Figure 10 and Equation 2) does not allow us to conclude that the presence of a black hole

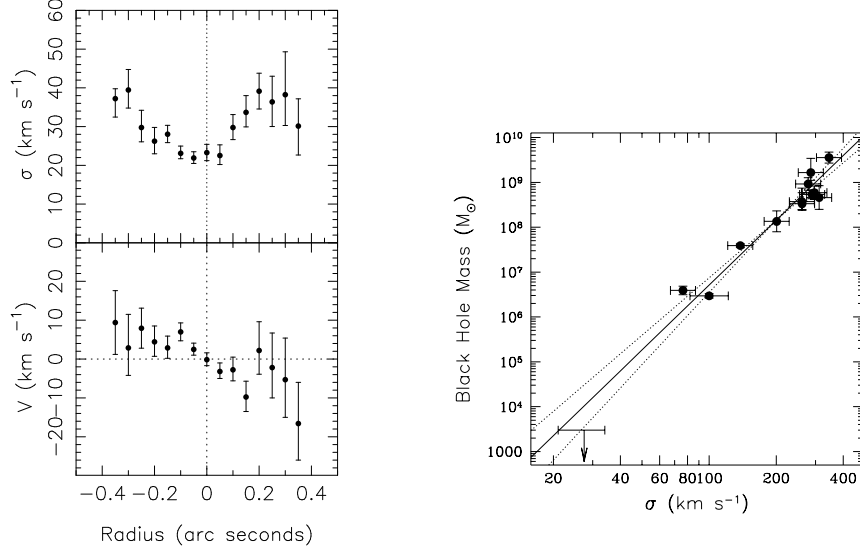


Figure 10. Upper limit on the mass of the black hole in M33 (adapted from Merritt, Ferrarese & Joseph 2001). Left: stellar rotation curve and velocity dispersion profile. Right: The $M_\bullet - \sigma$ relation including the upper limit on M_\bullet in M33.

in M33 would demand a formation mechanism different from the one responsible for the creation of supermassive black holes in other galaxies.

Can we expect to hear about the detection of $\leq 10^6 M_\odot$ nuclear black holes in galaxies other than M33 within the next few years? The remainder of this section discusses ongoing efforts and discusses what we are likely to learn.

4.2. Other New Data from HST

In the next few years, attempts will be made to detect and dynamically measure the masses of black holes at the centers of dozens of galaxies. The Space Telescope alone is committed to devoting several hundred orbits to the cause: roughly 130 galaxies have been or will be observed with STIS within the next two years as part of ~ 10 separate projects.

News from some of these projects is already starting to circulate. Sarzi *et al.* (2001) report results from an HST gas dynamical study of the nuclei of 24 nearby, weakly active galaxies. Four of the galaxies were found to have kinematics consistent with the presence of dust/gas disks (the prototype of which was detected in NGC 4261 by Jaffe *et al.* 1994); the authors conclude that in only one of the four galaxies (NGC 2787) can the kinematics provide meaningful constraints on the presence of a supermassive black hole. Barth *et al.* (2001) report the successful detection of a nuclear black hole in NGC 3245, one of six broad-lined AGNs targeted by the team with HST. The STIS Instrument Development Team (IDT) has obtained stellar absorption line spectra for ~ 12 galaxies and the data for the first of these, M32, have been published (Joseph

et al. 2001). The largest sample of stellar dynamical data (roughly 45 galaxies, about half of which have already been observed) will belong to the “Nuker” team. Data and a dynamical analysis have been published for one of these galaxies (NGC 3379, Gebhardt *et al.* 2001a) and preliminary masses for an additional 14 galaxies have been tabulated by Gebhardt *et al.* (2000b) and again by Kormendy & Gebhardt (2001). Mass estimates were apparently revised in the second tabulation, some by as much as 50%. We adopt the most recent values in the discussion that follows, pending publication of the full data and analyses.

We can update the $M_{\bullet} - \sigma$ relation using the additional black hole masses that have been published over the last year. In addition to the 12 galaxies used by Ferrarese & Merritt (2000) to define the $M_{\bullet} - \sigma$ relation, 10 galaxies listed in Table 1 also have $\text{FWHM}/2r_h < 1$. A regression fit accounting for errors in both coordinates (Akritas & Bershady 1996) to the expanded sample of 22 galaxies gives

$$M_{\bullet} = (1.48 \pm 0.24) \times 10^8 M_{\odot} \left(\frac{\sigma_c}{200 \text{ km s}^{-1}} \right)^{(4.65 \pm 0.48)} \quad (2)$$

in good agreement with previous determinations (Ferrarese & Merritt 2000; Merritt & Ferrarese 2001b). Within this sample, the two subsamples containing only stellar kinematical or stellar dynamical data produce fits with slopes of ~ 4.5 , in agreement with each other and with the slope quoted for the complete sample.

However, something interesting happens when the eight galaxies in Table 1 for which r_h has *not* been resolved are added to the sample (all of the mass determinations in these galaxies are based on stellar dynamics). Figure 11 shows the slope of the $M_{\bullet} - \sigma$ relation obtained from the stellar dynamical mass estimates when various cutoffs are placed on the quality of the data. If the complete sample is used (including all entries in Table 1 down to NGC 2778), the slope becomes quite shallow, 3.81 ± 0.33 . When only the best-resolved galaxies are included, $\text{FWHM}/r_h < 0.2$, the slope increases to 4.48 ± 0.12 , identical to the value obtained from the gas dynamical masses alone. Mass estimates based on the dynamics of gas disks are expected to be more accurate than estimates from stellar dynamics at equal resolution since the inclination angle of the disk can be measured and (if the motions are in equilibrium) the circular orbital geometry is simpler. From Figure 11, we conclude that the inclusion of masses derived from data that do not properly sample the black hole’s sphere of influence biases the slope of the relation. A similar conclusion was reached by Merritt & Ferrarese (2001b).

We also show in Figure 11 the results of least-squares fits using a simpler algorithm that does not account for measurement errors. This is the same algorithm used by Gebhardt *et al.* (2000a) (and presumably also by Kormendy & Gebhardt 2001). As pointed out by Merritt & Ferrarese (2001b), not accounting for measurements errors biases the slope too low: the inferred slope for the complete sample of stellar dynamical masses falls to ~ 3.5 using the simpler algorithm.

4.3. The Future

We noted above that a total of ~ 130 galaxies have been or will be observed with HST during the next two years with the hope of constraining the mass of

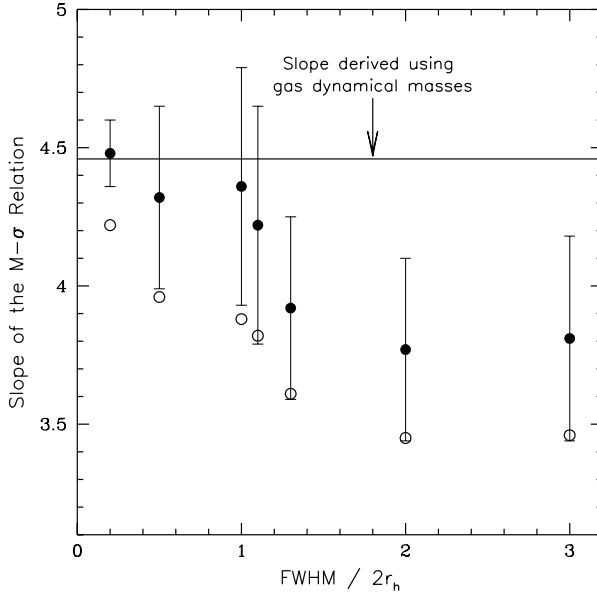


Figure 11. The slope of the $M_{\bullet} - \sigma$ relation as derived from stellar dynamical data as a function of data quality. Solid circles are slopes derived from a regression algorithm that accounts for errors in both variables; open circles are from a standard least-squares routine. Solid line is the slope derived from gas dynamical data, for which the black hole's sphere of influence was always resolved.

the central black hole. How many of these new data sets will in fact lead to stringent constraints on M_{\bullet} ? In Figure 2 we plot the expected radius of influence of the black hole versus $\text{FWHM}/2r_h$ for all galaxies for which a reliable distance (or redshift) and velocity dispersion could be gathered from the literature. Black hole masses have been estimated from the $M_{\bullet} - \sigma$ relation, Eq. (2). We argued above that the condition $\text{FWHM}/2r_h \geq 1.0$, compounded by the low S/N characteristic of HST data, will likely lead to weak constraints or biased determinations of M_{\bullet} , particularly in the case of stellar absorption line data.

Figure 1 shows that the black hole's sphere of influence will be resolved in less than half of these galaxies. Only one quarter will be resolved as well or better than NGC 3379 ($\text{FWHM}/2r_h \approx 0.4$), for which the constraints on M_{\bullet} are weak (§2.2). Among the galaxies slated to be observed in ionized gas, the preliminary results of Sarzi *et al.* (2001) suggest that few will be found to have the well-ordered disks that are necessary for secure estimates of M_{\bullet} .

Many of the “Sample A” galaxies from Ferrarese & Merritt (2000) were originally targeted for observation because of their exceptionally favorable properties, such as nearness (the Milky Way, M32), existence of a well-ordered maser disk (NGC 4258), etc. It is unlikely that many more galaxies will turn out to have equally favorable properties.

The majority of the targeted galaxies are expected to have black holes with masses of order $10^8 M_{\odot}$. This range is already well sampled by the current data; however the new detections might provide useful information about the scatter of the $M_{\bullet} - \sigma$ relation. Only a handful of black holes with masses \gtrsim

$10^9 M_\odot$ or a few $\times 10^7 M_\odot$ will be detected, and probably none in the $< 10^7 M_\odot$ range. Probing the low and high mass end of the $M_\bullet - \sigma$ relation is of particular interest since the slope and scatter of the relation have important implications for hierarchical models of galaxy formation (Haehnelt, Natarajan, & Rees 1998; Silk & Rees 1998; Haehnelt & Kauffmann 2000) and the effect of mergers on subsequent evolution (Cattaneo *et al.* 1999). The fact that the new observations will not appreciably extend the range of masses is not due to poor planning: the simple fact is that very small or very massive black holes are found in galaxies which are not close enough to resolve their sphere of influence using current optical/near infrared instrumentation.

It is our opinion that the future of the $M_\bullet - \sigma$ relation relies on methods other than traditional dynamical studies. An aggressive campaign to reverberation map a large sample of AGNs appears to be the obvious solution. The recent results from Ferrarese *et al.* (2001) show that reverberation mapping can produce mass estimates with a precision comparable to traditional dynamical studies. Although the obvious drawback is that it is only applicable to the 1% of galaxies with Type 1 AGN, reverberation mapping is intrinsically unbiased with respect to black hole mass, provided the galaxies can be monitored with the appropriate time resolution: while dynamical methods rely on the ability to spatially resolve the black hole's sphere of influence, reverberation mapping samples a region which is *per se* unresolvable. Furthermore, reverberation mapping can probe galaxies at high redshifts and with a wide range of nuclear activity, opening an avenue to explore possible dependences of the $M_\bullet - \sigma$ relation on redshift and activity level.

5. Origin of the $M_\bullet - \sigma$ Relation

The greatest dividend to come so far from the $M_\bullet - \sigma$ relation has been the resolution of the apparent discrepancy between black hole masses in nearby galaxies, the masses of black holes in AGN, and the mass density in black holes needed to explain quasar light. But the importance of the $M_\bullet - \sigma$ relation presumably goes beyond its ability to clarify the data. Like other tight, empirical correlations in astronomy, the $M_\bullet - \sigma$ relation must be telling us something fundamental about origins, and in particular, about the connection between black hole mass and bulge properties.

Probably the simplest way to relate black holes to bulges is to assume a fixed ratio of M_\bullet to M_{bulge} . Since $M_\bullet \propto \sigma^\alpha$ (Eq. 2), this assumption implies $M_{\text{bulge}} \propto \sigma^\alpha$. In fact this is well known to be the case: bulge luminosities scale as $\sim \sigma^4$, the Faber-Jackson law, and mass-to-light ratios scale as $\sim L^{1/4}$ (Faber *et al.* 1987), giving $M_{\text{bulge}} \sim \sigma^5$, in agreement with the slope $\alpha = 4.5 \pm 0.5$ derived above for the $M_\bullet - \sigma$ relation.

On the other hand, the $M_\bullet - \sigma$ relation appears to be much tighter than the relation between σ and bulge mass or luminosity. And even if a tight correlation between black hole mass and bulge mass were set up in the early universe, it is hard to see how it could survive mergers, which readily convert disks to bulges and may also channel gas into the nucleus, producing (presumably) uncorrelated changes in M_\bullet and M_{bulge} . The tightness of the $M_\bullet - \sigma$ relation suggests that some additional feedback mechanism acts to more directly connect black hole

masses to stellar velocity dispersions and to maintain that connection in spite of mergers.

One such feedback mechanism was suggested by Silk & Rees (1998) even before the discovery of the $M_\bullet - \sigma$ relation. These authors explored a model in which supermassive black holes first form via collapse of $\sim 10^6 M_\odot$ gas clouds before most of the bulge mass has turned into stars. The black holes created in this way would then accrete and radiate, driving a wind which acts back on the accretion flow. Ignoring star formation, departures from spherical symmetry etc., the flow would stall if the rate of deposition of mechanical energy into the infalling gas was large enough to unbind the protogalaxy in a crossing time T_D . Taking for the energy deposition rate some fraction f of the Eddington luminosity L_E , we have

$$f L_E T_D \approx \frac{GM_{\text{bulge}}^2}{R_{\text{bulge}}}. \quad (3)$$

Writing $GM_{\text{bulge}} \approx \sigma^2 R_{\text{bulge}}$, $T_D \approx R_{\text{bulge}}/\sigma$ and $L_E = 4\pi c GM_\bullet/\kappa$ with κ the opacity,

$$M_\bullet \approx f^{-1} \frac{\kappa \sigma^5}{4\pi G^2 c} \propto \sigma^5, \quad (4)$$

consistent with the observed relation. The constant of proportionality works out to be roughly correct if $f \sim 0.01 - 0.1$ (Silk & Rees 1998).

This model assumes that black holes acquire most of their mass during a fast accretion phase, $t_{\text{acc}} \lesssim 10^7$ yr. Kauffmann & Haehnelt (2000) developed a semi-analytic model for galaxy formation in which black holes grow progressively larger during galaxy mergers. The cooling of the gas that falls in during mergers is assumed to be partially balanced by energy input from supernovae. This feedback is stronger for smaller galaxies which has the effect of steepening the resulting relation between M_\bullet and σ . Haehnelt & Kauffmann (2000) found $M_\bullet \sim \sigma^{3.5}$ but the slope could easily have been increased if feedback effects had been increased (M. Haehnelt, private communication). However the scatter in the $M_\bullet - \sigma$ relation derived by them was only slightly less than the scatter in M_\bullet vs L_{bulge} , in apparent contradiction with the observations (Figure 1).

Burkert & Silk (2001) also considered a model in which black holes grow by accreting gas during mergers. In their model, accretion is halted when star formation begins to exhaust the gas in the outer accreting disk; the viscous accretion rate is proportional to σ^3 , and assuming a star formation time scale that is proportional to T_D , Burkert & Silk found $M_\bullet \propto R_{\text{bulge}} \sigma^2/G \propto M_{\text{bulge}}$, with a constant of proportionality that is again similar to that observed. This model does not give a convincing explanation for the tight correlation of M_\bullet with σ however.

Feedback of a very different sort was proposed by Norman, Sellwood & Hasan (1996), Merritt & Quinlan (1998) and Sellwood & Moore (1999). These authors simulated the growth of massive compact objects at the centers of barred or triaxial systems and noted how the nonaxisymmetric component was weakened or dissolved when the central mass exceeded a few percent of the stellar mass. Since departures from axisymmetry are believed to be crucial for channelling gas into the nucleus, the growth of the black hole has the effect of cutting off its own supply of fuel. These models, being based purely on stellar dynamics, have the nice feature that they can be *falsified*, and in fact they probably

have been: our new understanding of black hole demographics (§2,3) suggests that few if any galaxies have $M_\bullet/M_{\text{bulge}}$ as great as 10^{-2} . (At the time of these studies, several galaxies were believed from ground-based data to have $M_\bullet/M_{\text{bulge}} > 1\%$, including NGC 1399 (Magorrian *et al.* 1998), NGC 3115 (Kormendy *et al.* 1996a), and NGC 4486b (Kormendy *et al.* 1997)).

The tightness of the $M_\bullet - \sigma$ relation must place strong constraints on the growth of black holes during mergers. We know empirically that mergers manage to keep galaxies on the fundamental plane, which is a relation between σ , the bulge radius R_e and bulge luminosity L . The σ that appears in the fundamental plane relation is the same σ_c that appears in the $M_\bullet - \sigma$ relation (indeed, it was defined by Ferrarese & Merritt 2000 for just this reason) and furthermore σ_c is defined within a large enough aperture that it is unlikely to be significantly affected by dynamical processes associated with the formation of a black-hole binary during a merger (Milosavljevic & Merritt 2001). Hence the physics of the black-hole binary can be ignored and we can ask simply: How do mergers manage to grow black holes in such a way that $\Delta \log M_\bullet \approx 4.5 \Delta \log \sigma$, independent of changes in R_e and L ?

References

Akritas, M. G. & Bershady, M. A. 1996, ApJ, 470, 706
 Arav, N. *et al.* 1997, MNRAS, 288, 1015
 Arav, N. *et al.* 1998, MNRAS, 297, 990
 Bacon, R. *et al.* 2001, A&A, 371, 409
 Barger, A. J. *et al.* 2001, AJ, 121, 662
 Barth, A. J., Sarzi, M., Rix, H.-W., Ho, L. C., Filippenko, A. V. & Sargent, W. L. W. 2001, astro-ph/0012213
 Blandford, R. D. & McKee, C. F. 1982, ApJ, 255, 419
 Bower, G. A. *et al.* 1998, ApJ, 492, L111
 Braatz, J. A., Wilson, A. S. & Henkel, C. 1996, ApJS, 106, 51
 Burkert, A. & Silk, J. 2001, ApJ, 554, 151
 Cattaneo, A., Haehnelt, M. G. & Rees, M. J. 1999, MNRAS, 308, 77
 Chokshi, A. & Turner, E. L., 1992, MNRAS, 259, 421
 Collin-Souffrin, S., Dyson, J. E., McDowell, J. C. & Perry, J. J. 1988, MNRAS, 232, 539
 Cretton, N. & van den Bosch, F.C. 1999, ApJ, 514, 704
 Dehnen, W. 1993, MNRAS, 265, 250
 Dietrich, M. *et al.* 1999, A&A, 351, 31
 Emsellem, E., Dejonghe, H. & Bacon, R. 1999, MNRAS, 303, 495
 Fabbiano, G., Zeza, A. & Murray, S. S. 2001, astro-ph/0102256
 Faber, S. *et al.* 1987, in *Nearly Normal Galaxies*, ed. S. Faber (Springer: New York), 175
 Faber, S. 1999, Advances in Space Research, 23, 925
 Fabian, A. C. & Iwasawa, K. 1999, MNRAS, 303, L34

Ferland, G. J. *et al.* 1992, ApJ, 387, 95

Ferrarese, L. & Ford, H.C. 1999, ApJ, 515, 583

Ferrarese, L., Ford, H.C. & Jaffe, W. 1996, ApJ, 470, 444

Ferrarese, L. & Merritt, D. 2000, ApJ, 539, L9

Ferrarese, L., Pogge, R. W., Peterson, B. M., Merritt, D., Wandel, A. & Joseph, C. M. 2001, astro-ph/0104380

Ferrarese, L. *et al.* 2000, ApJ, 529, 745

Gebhardt, K. *et al.* 2000a, AJ, 119, 1157

Gebhardt K. *et al.* , 2000b, ApJ, 539, L13

Genzel, R., Pichon, C., Eckart, A., Gerhard, O. E. & Ott, T. 2000, MNRAS, 317, 348

Ghez, A. M., Klein, B. L., Morris, M. & Becklin, E. E. 1998, ApJ, 509, 678

Greenhill, L. J. *et al.* 1995, ApJ, 440, 619

Greenhill, L. J., Gwinn, C. R., Antonucci, R. & Barvainis, R. 1996, ApJ, 472, L21

Greenhill, L. J., Moran, J. M. & Herrnstein, J. R. 1997, ApJ, 481, L23

Haehnelt, M. G. & Kauffmann, G. 2000, MNRAS, 318, L35

Haehnelt, M. G., Natarajan, P. & Rees, M. J. 1998, MNRAS, 300, 817

Herrnstein, J. R. *et al.* 1999, Nature, 400, 539

Ho, L. C. 1999, in Observational Evidence for Black Holes in the Universe, ed. S. K. Chakrabarti (Dordrecht: Reidel), 157

Jaffe, W., Ford, H. C., O'Connell, R. W., van den Bosch, F. C. & Ferrarese, L. 1994 AJ, 108, 1567

Joseph, C. *et al.* 2001, ApJ, 550, 668

Kaspi, S., Smith, P. S., Maoz, D., Netzer, H. & Jannuzi, B. T. 1996, ApJ, 471, L75

Kaspi, S., Smith, P.S., Netzer, H., Maoz, D., Jannuzi, B.T., & Giveon, U. 2000, ApJ, 533, 631

Kauffmann, G. & Haehnelt, M. 2000, MNRAS, 311, 576

Koratkar, A. P. & Gaskell, C. M. 1991, ApJS, 75, 719

Kormendy, J. *et al.* 1996a, ApJ, 459, L57

Kormendy, J. *et al.* 1996b, ApJ, 473, L91

Kormendy, J. *et al.* 1997, ApJ, 482, L139

Kormendy, J. *et al.* 1998, AJ, 115, 1823

Kormendy, J. & Gebhardt, K. 2001, astro-ph/0105230

Kormendy, J. & McClure, D. 1993, AJ, 105, 1793

Krolik, J. 2001, astro-ph/0012134

Laor, A. 1998, ApJ, 505, L83

Laor, A. 2001, astro-ph/0101405

Macchetto, F., *et al.* 1997, ApJ, 489, 579

Magorrian, J. *et al.* 1998, AJ, 115, 2285

Malkan, M. A., Gorjian, V. & Tam, R. 1998, ApJS, 117, 25

Maoz, E. *et al.* 1999, *Nature*, 401, 351

Marconi, A. *et al.* 2001, *ApJ*, 549, 915

Mathur, S. *et al.* 2001, *astro-ph/0104263*

Matsumoto, H. *et al.*, *ApJ*, 547, L25

McLure, R. J. & Dunlop, J. S. 2000, *astro-ph/0009406*

Merrifield, M. R., Forbes, D. A. & Terlevich, A. I. 2000, *MNRAS*, 313, L29

Merritt, D. 1994, in *Clusters of Galaxies, Proceedings of the 29th Rencontre de Moriond*, ed. F. Durret, A. Mazure & J. Tran Thanh Van (Singapore: Editions Frontieres), 11

Merritt, D. & Ferrarese, L. 2001a, *MNRAS*, 320, L30

Merritt, D. & Ferrarese, L. 2001b, *ApJ*, 547, 140

Merritt, D., Ferrarese, L. & Joseph, C. 2001, submitted

Merritt, D. & Quinlan, G. D. 1998, *ApJ*, 498, 625

Miller, M. C. & Hamilton, D. P. 2001, *astro-ph/0106188*

Milosavljevic, M. & Merritt, D. 2001, *astro-ph/010350*

Miyoshi, M. *et al.* 1995, *Nature*, 373, 127

Murry, N. & Chiang, J. 1997, *ApJ*, 474, 91

Murray, N., Chiang, J., Grossman, S. A. & Voit, G. M. 1995, *ApJ*, 451, 498

Nelson, C. H. & Whittle, M. 1995, *ApJS*, 99, 67

Netzer, H. & Peterson, B. M. 1997, in *Astronomical Time Series*, ed. D. Maoz, A. Sternberg, & E.M. Leibowitz, (Dordrecht: Kluwer), 85

Neugebauer, C. *et al.* 1987, *ApJS*, 63, 615

Newman, J.A. *et al.* 2001, *ApJ*, 553, 562

Norman, C. A., Sellwood, J. A. & Hasan, H. 1996, *ApJ*, 462, 114

Osterbrock, D. E. & Pogge, R. W. 1985, *ApJ*, 297, 166

Pelletier, G. & Pudritz, R. E. 1992, *ApJ*, 394, 117

Peterson, B. M. 1993, *PASP*, 105, 247

Peterson, B. M. & Wandel, A. 2000, *ApJ*, 540, L13

Richstone, D. O. *et al.* 1998, *Nature*, 395, A14

Richstone, D. O., Bower, G. & Dressler, A. 1990, *ApJ*, 353, 118

Salpeter, E. E. 1964, *ApJ*, 140, 796

Salucci, P. *et al.* 1999, *MNRAS*, 307, 637

Sarzi, M. *et al.* 2001, *astro-ph/0012406*

Sellwood, J. A. & Moore, E. M. 1999, *ApJ*, 510, 125

Silk, J. & Rees, M. J. 1998, *A&A*, 331, L4

Simien, F. & de Vaucouleurs, G. 1986, *ApJ*, 302, 564

Soltan, A. 1982, *MNRAS*, 200, 115

Smith, M. D. & Raine, D. J. 1985, *MNRAS*, 212, 425

Smith, M. D. & Raine, D. J. 1988, *MNRAS*, 234, 297

Tonry, J. L. 1984, *ApJ*, 283, L27

Tonry, J. L., *et al.* 2001, *ApJ*, 546, 681

Trotter, A. S. *et al.* 1998, ApJ, 495, 740

van der Marel, R. P. 1997, in Galaxy Interactions at Low and High Redshift, Proc. IAU Symp. 186 (Kluwer: Dordrecht)

van der Marel, R. P. & van den Bosch, F. C. 1998, AJ, 116, 2220

Verdoes Kleijn, G.A., van der Marel, R., Carollo, C. M. & de Zeeuw, P. T. 2000, AJ, 120, 1221

Véron-Cetty, M.-P., Véron, P. & Goncalves, A. C. 2001, A&A, 372, 730

Wandel A., 1999, ApJ, 519, 39

Wandel, A., Peterson, B. M. & Malkan, M.A. 1999, ApJ, 526, 579

Watson, W. D. & Wallin, B. K. 1994, ApJ, 432, 35

Whittle, M. *et al.* 1992, ApJS, 79, 49

Zeldovich, Ya. B. 1964, Soviet Physics - Doklady, 9, 195